

## Auroral Current and Electrodynamics Structure (ACES) observations of ionospheric feedback in the Alfvén resonator and model responses

I. J. Cohen,<sup>1</sup> M. R. Lessard,<sup>1</sup> S. R. Kaeppler,<sup>2</sup> S. R. Bounds,<sup>2</sup> C. A. Kletzing,<sup>2</sup>  
 A. V. Streltsov,<sup>3</sup> J. W. LaBelle,<sup>4</sup> M. P. Dombrowski,<sup>4</sup> S. L. Jones,<sup>5</sup> R. F. Pfaff,<sup>5</sup>  
 D. E. Rowland,<sup>5</sup> B. J. Anderson,<sup>6</sup> H. Korth,<sup>6</sup> and J. W. Gjerloev<sup>6,7</sup>

Received 19 December 2012; revised 15 May 2013; accepted 16 May 2013; published 21 June 2013.

[1] The ACES-High rocket, part of the Auroral Current and Electrodynamics Structure (ACES) mission launched from Poker Flat Research Range on 29 January 2009, obtained the first in situ measurements indicative of both of the observational characteristics associated with the ionospheric feedback instability as it flew through an auroral arc and its associated return current region. ACES-High observed Alfvénic wave structures localized in areas of roughly 10 km near the boundaries of the return current region associated with the discrete auroral arc and increased electron density with a temperature characteristic of a cold ionosphere. This density enhancement is believed to be caused by the excavation of plasma from lower altitudes via the ponderomotive force produced by the ionospheric Alfvén resonator, as shown by Streltsov and Lotko (2008). While this density is lower than expected from simulations and other observations by as much as an order of magnitude, the ratio of the enhancement to the background density is in agreement with predictions. The observations made by ACES-High agree with the model results by Streltsov and Lotko (2008) but show the localized wave structures only near the boundaries of the return current region and not throughout it. This can be explained by strong small-scale magnetic field-aligned currents that are generated by the interaction between the large-scale downward current and the ionosphere at these boundaries. Finally, a new model, based on that by Streltsov and Marklund (2006), was run with only one downward current region and produced results very similar to the observations seen by ACES-High.

**Citation:** Cohen, I. J., et al. (2013), Auroral Current and Electrodynamics Structure (ACES) observations of ionospheric feedback in the Alfvén resonator and model responses, *J. Geophys. Res. Space Physics*, 118, 3288–3296, doi:10.1002/jgra.50348.

### 1. Introduction

[2] The ionospheric feedback instability (IFI) was first introduced by Atkinson [1970] as a system model to explain the processes that drive auroral arcs. The model, illustrated

qualitatively in Figure 3 of that paper, assumes a change in ionospheric conductivity to start. This perturbation of the conductivity creates electric fields in the ionosphere that then map to the magnetosphere. A flux tube in the magnetosphere would then see a time-varying magnetospheric electric field which drives polarization currents that produce field-aligned currents (FACs) to close the current loop. The upward FAC is characterized by downward precipitating electrons that cause the ionospheric conductivity variations that are assumed at the start, thereby closing the feedback loop.

[3] Two key observational characteristics of the IFI are low-altitude plasma density depletions and small-scale electromagnetic waves located in the vicinity of discrete auroral arcs. Observations from sounding rockets, ground-based radars, and satellites have shown evidence of plasma density depletions in the ionosphere and the low-altitude magnetosphere adjacent to magnetic FAC regions [Doe et al., 1993; Shepherd et al., 1998; Aikio et al., 2004]. Streltsov et al. [2011] shows two examples of strong ionospheric density depletion in a localized region next to the region where it is enhanced by auroral precipitation. The significant presence

<sup>1</sup>Space Science Center, University of New Hampshire, Durham, New Hampshire, USA.

<sup>2</sup>Department of Physics and Astronomy, University of Iowa, Iowa City, Iowa, USA.

<sup>3</sup>Department of Physical Sciences, Embry-Riddle Aeronautical University, Daytona Beach, Florida, USA.

<sup>4</sup>Department of Physics and Astronomy, Dartmouth College, Hanover, New Hampshire, USA.

<sup>5</sup>NASA Goddard Space Flight Center, Greenbelt, Maryland, USA.

<sup>6</sup>Space Department, Johns Hopkins University Applied Physics Laboratory, Laurel, Maryland, USA.

<sup>7</sup>Department of Physics and Technology, University of Bergen, Bergen, Norway.

Corresponding author: I. J. Cohen, Space Science Center, University of New Hampshire, Morse Hall, 8 College Road, Durham, NH 03820, USA. (ian.cohen@unh.edu)

of intense ULF waves in the downward current channels has also been demonstrated by a number of observations from satellites [Paschmann *et al.*, 2003; Mishin *et al.*, 2003] and on the ground [Streltsov *et al.*, 2010].

[4] Later theoretical studies of ionospheric feedback built upon the model proposed by Atkinson [1970] and supplied quantitative information about structure in the vicinity of auroral arcs, caused by interactions between pairs of downward and upward magnetic FACs and the ionosphere [Streltsov and Lotko, 2003a, 2003b, 2008]. Streltsov and Lotko [2003b] present results from a numerical study of the origin and spatiotemporal properties of such intense, small-scale electromagnetic structures observed in the vicinity of discrete auroral arcs by low-altitude, polar-orbiting satellites. Their results show that these small-scale electromagnetic (EM) structures can be produced inside the ionospheric Alfvén resonator (IAR), a cavity formed by the E-layer of the ionosphere at the bottom and the increase in Alfvén speed at the top. Streltsov and Lotko [2003b] presents three primary effects of FAC in creating and maintaining the resultant IFI: (a) the removal of electrons from the ionosphere in the downward FAC locally decreases the ionospheric conductance and lowers the threshold for IFI, (b) a Pedersen current closing the FAC enhances the perpendicular electric field in the E-layer and creates even more favorable conditions for the IFI, and (c) a resistive layer in the lower magnetosphere is produced by the FAC that provides a well-defined upper boundary for the IAR, confining the small-scale feedback-amplified Alfvén waves.

[5] The hypothesis that low-altitude density cavities in the downward current channels can be caused by small-scale, intense shear Alfvén waves, thus linking the two characteristics of the IFI, was investigated numerically by Streltsov and Lotko [2008] and Sydorenko *et al.* [2008]. In particular, Streltsov and Lotko [2008] produced numerical results based on a reduced two-fluid MHD model that self-consistently describes shear Alfvén waves, ion parallel dynamics, effects of the ionospheric E-region activity, and the magnetosphere-ionosphere feedback instability. These numerical simulations were performed in a dipole magnetic field geometry with realistic parameters of the ambient plasma. Figure 1 shows the results of the numerical model by Streltsov and Lotko [2008]. Figure 1a shows the geometry of the initial conditions, where two oppositely directed (upward and downward) FACs are launched. Figure 1b shows the formation of the small-scale EM structures within the downward FAC region. The small-scale structure is seen throughout most of the return current region, with a higher population at the boundary between the upward and downward FACs. Figure 1c shows how the upward evacuation of plasma from low altitudes causes a density cavity with a density enhancement above it. The dashed line traces a rough estimate of the trajectory of the ACES-High rocket. At the apogee altitude of ACES-High, the rocket would miss the plasma density cavity predicted by the model and fly through the density enhancement that is created above the cavity. Figure 1d shows the ion outflow velocity. Streltsov and Lotko [2008] showed that the ponderomotive force created by the IAR alone can cause a decrease of up to 96% of the background magnitude of plasma density between the E and F regions. They also reasoned that the density depletion would cover a large part of the downward FAC region. The

cavity formation presented by Streltsov and Lotko [2008] generally agrees with, but has a much lower observed ion temperature than, the ground-based radar observations by Aikio *et al.* [2004]. Temporal aspects of the feedback process depend on parameters of the background ionospheric plasma (density, temperature, recombination rate, etc.) and on the magnitude of the large-scale electric field in the ionosphere. Streltsov and Lotko [2008] showed that for typical parameters of the magnetosphere-ionosphere system in the auroral zone (plasma density  $3 \times 10^4 \text{ cm}^{-3}$ , Pedersen conductivity  $\sim 2 \text{ mho}$ , perpendicular electric field  $\sim 100 \text{ mV/m}$ , and the parallel current density  $\sim 10 \text{ } \mu\text{A/m}^2$ ), the instability reaches saturation within 60 s.

[6] The model did not reproduce the elevated ion temperature in the cavity nor include the effects of this heating on the ion parallel motion since it included only an isothermal treatment of the ion population. The simulation results also show that the ratio between the height integrated ionospheric Pedersen conductivity,  $\Sigma_p$ , and the Alfvén conductivity in the near-Earth magnetosphere defined as  $\Sigma_A = 1/\mu_0 v_A$  (where  $v_A = B_0/\sqrt{\mu_0 \rho}$  is the Alfvén speed,  $B_0$  is the background magnetic field, and  $\rho$  is the mass density) is an important parameter for the production of the necessary small-scale, intense ULF waves at low altitudes. Theoretical studies have shown that the maximization of the growth rate of IFI occurs when  $\Sigma_p \approx \Sigma_A$  [Lysak, 1991; Pokhotelov *et al.*, 2001; Lysak and Song, 2002]. Streltsov *et al.* [2011] explain that when  $\Sigma_p \approx \Sigma_A$  a “matching impedance” condition exists between the ionosphere and magnetosphere where waves can propagate from one layer into the other, with the condition determined by the mass density near the ionosphere—a parameter that may fluctuate as ions move along the magnetic field lines.

## 2. Observations

[7] The ACES rockets were launched into a dynamic multiple-arc aurora from Poker Flat Research Range in Alaska on 29 January 2009. The two-rocket mission was designed to investigate the three-dimensional current geometry of the auroral environment. The apogee of the ACES-High rocket (365 km) was such that it allowed the instrument payload to pass through both the upward and downward current regions of a discrete arc at an altitude where collisional effects between ions and neutrals has a negligible influence on the electrodynamics of the system. The ACES-High scientific payload was equipped with a fluxgate magnetometer, a pair of Electron Retarding Potential Analyzers (ERPAs), a pair of Langmuir probes cross calibrated with an HF receiver, double probes to measure the perpendicular DC electric field and low-frequency wave activity, and a top hat electrostatic analyzer for the electrons. Further details regarding observations made by the ACES mission can be found in Kaeppler *et al.* [2012].

[8] Figure 2 shows data from the ACES-High rocket as it passed, in a northward/poleward trajectory, through a stable auroral arc at roughly 350 km altitude (just above the F region peak) at approximately 1 km/s on the morning of 29 January 2009. Figure 2a shows the average brightness of several pixels within a given latitude/longitude range of the payload footprint. To obtain this trace, the spacecraft’s coordinates and the coordinates of the individual

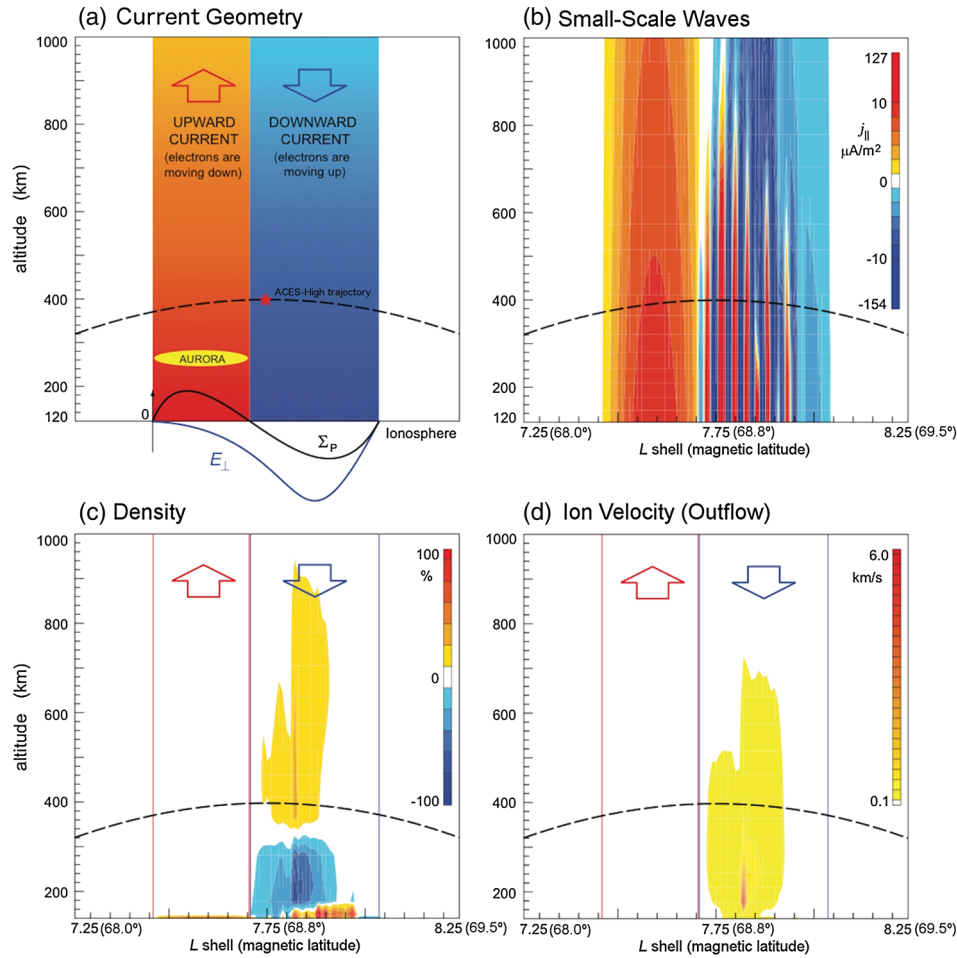


**Figure 1.** Results from numerical simulations by *Streltsov and Lotko* [2008]. Figure 1a shows the geometry of the initial conditions, where two oppositely directed (upward and downward) FACs are launched. Figure 1b shows the formation of the small-scale EM structures within the downward FAC region. Figure 1c shows how the upward evacuation of plasma from low altitudes causes a density cavity with a density enhancement above it. Figure 1d shows the ion outflow velocity. The dashed line traces a rough estimate of the trajectory of the ACES-High rocket.

pixels of the all-sky imager assuming emissions at 110 km were converted to Altitude Adjusted Corrected Geomagnetic coordinates. Then, the coordinates of the all-sky grid were matched with the coordinates of the payload, and the average brightness was taken over a range of  $\pm 0.02$  in latitude and  $\pm 0.05$  in longitude of the payload footprint. The small periodic peaks that occur from 09:54:00 UTC onward are the result of noise from the video recording device. This device created a visible bar of brightness that can be seen scrolling down the field of view in each subsequent frame. The peak in this panel, at around 09:53:41 UTC, indicates the location of the visible discrete auroral arc associated with the upward current region as shown by the FAC measurements in Figure 2b. The FACs were derived from magnetometer data by taking the spatial derivative and implementing Ampere's law, assuming that the spacecraft is moving fast relative to the current structures to allow the application of the Taylor Hypothesis and convert temporal into spatial structures. Finally, a median filter (of approximately 0.5 s) was applied to the output current data to get the overall FAC structure. Note that the field-aligned currents measured were

on order of tens of  $\mu\text{A}/\text{m}^2$ , on the lower end of the range of 10–127  $\mu\text{A}/\text{m}^2$  predicted by *Streltsov and Lotko* [2008].

[9] Figure 2c shows the pitch angle distribution of the electron flux at 164 eV. Figure 2d depicts the differential electron energy flux in the range of 80–500 eV. Figures 2e and 2f display the meridional and zonal electric fields. This study primarily focuses on the region between 09:53:56 UTC and 09:54:19 UTC. This time period outlines a decrease in electron flux, bounded by strong signatures of Alfvénic precipitation (characterized by a field-aligned population over a broad distribution of energy from 0 to a few hundreds of eV). The electron flux recorded here is similar to the time-dispersed signatures from the model and data presented by *Kletzing and Hu* [2001]. They showed that time-dispersed signatures of this type could be generated by propagating Alfvénic pulses along realistic field lines. Observation of these features by ACES-High suggests that use of the Alfvén resonator model is appropriate to understand our data.

[10] Associated with this Alfvénic activity are electromagnetic perturbations seen in Figures 2e and 2f. It is

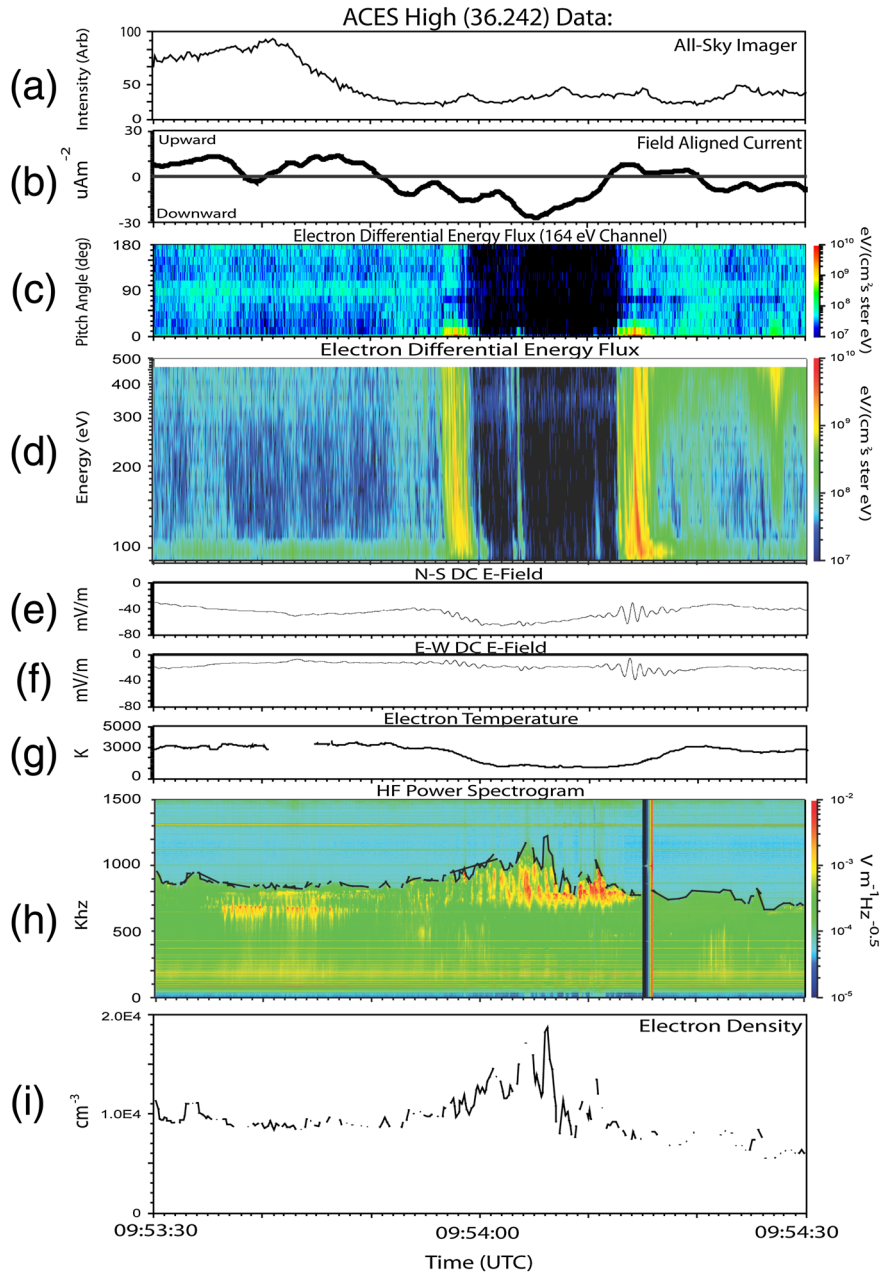


**Figure 2.** Data from the ACES-High rocket as it passed, in a northward/poleward trajectory, through a stable auroral arc at roughly 350 km altitude (just above the F region peak) at approximately 1 km/s on the morning of 29 January 2009. Figure 2a shows the average brightness of several pixels within a given latitude/longitude range of the payload footprint, which peaks around 09:53:41 UTC. This peak indicates the location of the visible discrete auroral arc associated with the upward current region as shown in Figure 2b, which shows the FAC. Figure 2c shows the field-aligned pitch angle distribution of the electron flux at 164 eV. Figure 2d depicts the differential electron energy flux in the range of 80–500 eV, providing clear evidence of a broad energy distribution characteristic of Alfvénic precipitation. Figures 2e and 2f display the meridional and zonal electric fields. Figures 2g, 2h, and 2i show the electron temperature, high frequency power spectrum, and electron density, respectively.

important to note that although these perturbations look to have roughly 1 Hz frequency, we cannot necessarily characterize them as such due to limitations in temporal and spatial information. Although we cannot make strong conclusions about the spatial characteristics of the waves, we use the term “small-scale” to refer to these waves that appear to be localized in a region of roughly 10 km,

comparable to the length scales of interest for FAC (of order 1–10 km). Note that both the EM wave magnitude and electron flux are greater at the poleward event than the equatorward one. Figures 2g, 2h, and 2i show the electron temperature, high frequency (HF) power spectrum, and electron density derived from the HF, respectively. These results do echo the predictions of enhanced electron density in the

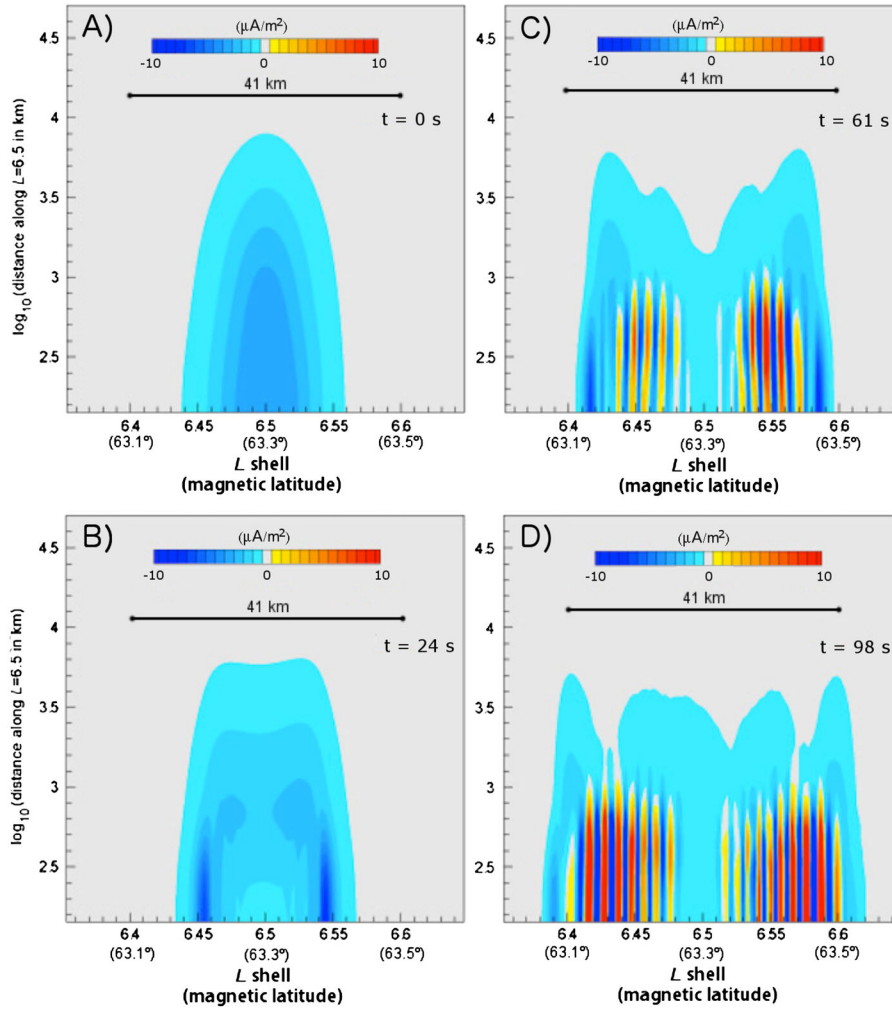


**Figure 3.** Results from a new model similar to the one described in detail by *Streltsov and Marklund* [2006] with a few minor parameter changes. This simulation included only a single downward FAC region, as opposed to the two oppositely directed FACs included in the simulations by *Streltsov and Lotko* [2008]. The small-scale electromagnetic oscillations seen in the results from the new model are on the order of  $10 \mu\text{A}/\text{m}^2$ , of the same order as the field-aligned current measured by ACES-High (see Figure 2b).

downward current region at altitudes above 340 km caused by the upward movement of the ionosphere in response to the ponderomotive force created by the intense ULF waves [*Streltsov and Lotko*, 2004, 2008; *Streltsov et al.*, 2011]. However, the overall densities observed are relatively low. The electron temperature in Figure 2g, obtained by the ERPA instrument, confirms that the density enhancement occurs in a return current region with a characteristic temperature of a cold ionosphere (fractions of an eV).

### 3. Model Response

[11] As evidenced in Figures 2e–2f, the intense small-scale electromagnetic waves seen at the boundaries of the downward FAC region by ACES-High are not present throughout the FAC region, as was predicted by the original simulations from *Streltsov and Lotko* [2008]. In response to this new data, the model was reconfigured, and new

simulations were run. The physical model, its numerical implementation, and simulation domain used in this study are similar to the ones described in detail by *Streltsov and Marklund* [2006] with a few minor parameter changes.

[12] As in *Streltsov and Marklund* [2006], the domain of this model is comprised of a dipolar flux tube, bounded by the ionosphere at the bottom and extending to the equatorial plane. Here the simulation domain is bounded in latitude by the  $L = 6.35$  and  $L = 6.65$  dipole magnetic shells and the magnetic field at the  $L = 6.5$  (center) shell at the equator is 112.9 nT. As illustrated in Figure 2 of *Streltsov and Lotko* [2003a], at the equatorial plane, a cylindrical extension is added on top of the dipole part of the model domain allowing a “buffer” zone which eliminates the effects of the artificial reflections from the magnetospheric end of the domain on the electrodynamics of the low-altitude region during the “buffer” time. In this model, the cylindrical extension is  $27.8 R_E$ , the Alfvén speed in the cylinder is 3176.9 km/s, and the plasma density at the equatorial

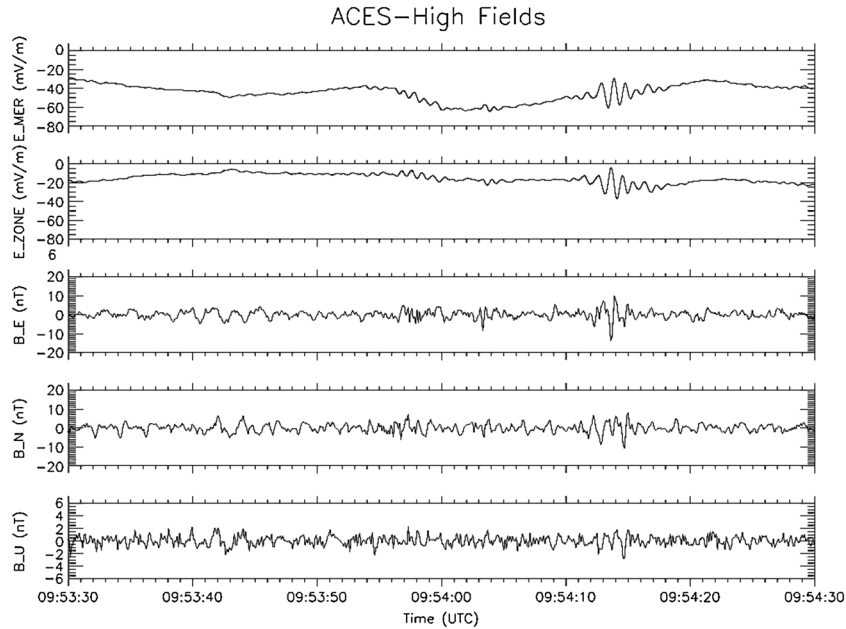


**Figure 4.** The electric and magnetic field measurements taken from ACES-High as it passed through the upward and downward current regions associated with a stable auroral arc at roughly 1 km/s. Particularly of interest were the small-scale electromagnetic waves seen at the equatorward and poleward boundaries of the downward current region, appearing at roughly 09:53:58 UTC and 09:54:15 UTC.

magnetosphere is  $0.6 \text{ cm}^{-3}$ . This model's "buffer" time, as the wave propagates through the cylindrical extension, of  $(2 \times 27.8 R_E \times 6371.2 \text{ km}) / 3176.9 \text{ km/s} = 111.5 \text{ s}$ . Unlike the model used by *Streltsov and Marklund* [2006], the model introduced here also includes correction to the Alfvén speed at low altitudes due to the presence of heavy ions ( $\text{O}_2^+$  and  $\text{NO}^+$ ) in the ionosphere.

[13] The results from the new simulations are shown in Figure 3. Note, as previously detailed, that this simulation decoupled the FAC regions by including only a single downward FAC region, as opposed to the two oppositely directed FACs included in the simulations by *Streltsov and Lotko* [2008]. Note that the small-scale oscillations seen in the results from the new model are on the order of  $10 \mu\text{A/m}^2$ , of the same order as the field-aligned current measured by ACES-High (see Figure 2b). The small-scale oscillations are better visualized in the FACs since the differentiation done to obtain them serves as a high-pass filter, eliminating the large-scale, smooth characteristics of the magnetic field. As Figures 3c and 3d show, the intense small-scale oscillations are only seen near the boundaries of the downward current region. This is similar to the observations made by ACES-High but differ from the results of *Streltsov and Lotko* [2008] where the oscillations were seen strongly at the boundary between the upward and downward current regions and existed throughout most of the downward current region. The electron precipitation and electromagnetic waves are generated near the boundaries of the large-scale downward current (see Figures 2c–2f) because the strongest small-scale magnetic FACs are generated by the interaction between the large-scale downward current and the ionosphere. The fact that the results of the new model are in much better agreement with the data obtained by ACES-High seems to imply that the FAC regions may in fact be decoupled.

## 4. Analysis

### 4.1. Field Polarity

[14] Figure 4 shows the electric and magnetic field measurements taken by ACES-High as it passed through the upward and downward current regions. Of particular interest are the small-scale electromagnetic waves seen at the equatorward and poleward boundaries of the downward current region, appearing at roughly 09:53:58 UTC and 09:54:15 UTC. If the small-scale EM waves observed by ACES-High are standing waves, formed by reflections at the boundaries of the IAR, then we would expect to see a  $90^\circ$  phase shift between the electric and magnetic fields that is characteristic of standing waves. To analyze the polarity of the EM waves, a Hilbert transform was applied to the magnetic field component of the wave, introducing a  $90^\circ$  phase shift at all frequencies. Figure 5 shows a comparison of the electric field component (dashed line) with the Hilbert transformed magnetic field component (solid line) which illustrates a phase difference of roughly  $20^\circ$ . Since a  $90^\circ$  phase shift was introduced to the magnetic component of the wave by the Hilbert transform, the waves would show no phase difference if they were precisely  $90^\circ$  out of phase with one another before the transform. The analysis shows that the electric and magnetic components of the Alfvén wave observed have a phase difference that is not equal to  $90^\circ$  and are not pure standing waves.

[15] *Knudsen et al.* [1992] compared observations of fields measured by auroral sounding rockets and data from polar-orbiting satellites (including HILAT) to limiting-case models to explain low-frequency field fluctuations seen by low-altitude spacecraft. They found that the sounding rocket data were in excellent agreement with the standing Alfvén wave model, while the data from the satellites were in better agreement with the static current model. They proposed

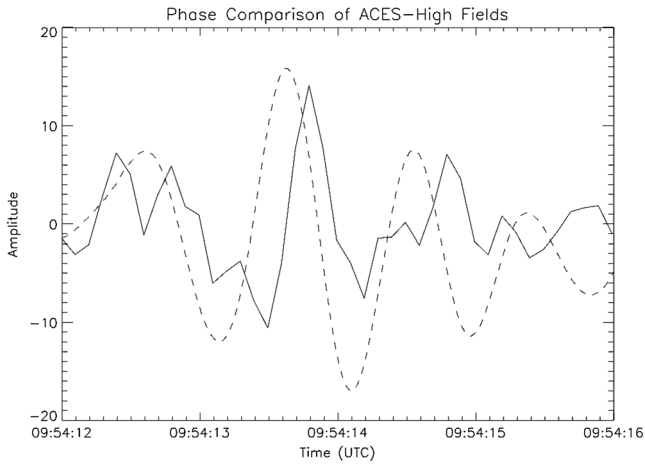


**Figure 5.** Comparison of the electric field component (dashed line) with the Hilbert transformed magnetic field component (solid line) shows an apparent phase difference of roughly  $20^\circ$ . Since a  $90^\circ$  phase shift was introduced to the magnetic component of the wave by the Hilbert transform, the waves would show no apparent phase difference if they were precisely  $90^\circ$  out of phase with one another before the transform. This analysis shows clearly that the electric and magnetic components of the Alfvénic wave observed have a phase difference that is neither  $0^\circ$ ,  $90^\circ$ , nor  $180^\circ$ .

two explanations, based around the movement and trajectory of the rocket, for the inconsistencies. *Clemmons et al.* [2000] reported in their measurements of ULF waves from the Polar satellite that the electric and magnetic field signatures were nearly in phase, differing by only about  $20^\circ$ , similar to the phase difference seen in our analysis. They claim that such a wave is actually best characterized as a traveling wave with a small admixture of a standing wave. ACES-High observed a phase difference between the electric and magnetic fields that was not equal to  $90^\circ$ , most likely attributable to the IAR's imperfections as a resonant cavity. The observed phase difference suggests that these waves are not true standing waves, but most likely a standing wave mixed with a traveling wave as *Clemmons et al.* [2000] described.

#### 4.2. Electron Flux, Density, and Temperature

[16] The electron density data plotted in Figure 2i show density values of  $1.3\text{--}1.8 \times 10^4 \text{ cm}^{-3}$ , which are 3–10 times less than the lowest densities seen at 350 km in the European Incoherent Scatter radar data from *Aikio et al.* [2004] and an order of magnitude lower than the results of the numerical model presented by *Streltsov et al.* [2011]. The results from both of these studies, and the predictions from *Streltsov and Lotko* [2008], predict that at an altitude of 350 km ACES-High should have flown through the density enhancement region produced by the evacuation of plasma from the cavity that is created below it. ACES-High did see a local enhancement of electrons in the heart of the downward current region, but the overall densities measured were still up to an order of magnitude lower than expected. Figure 1c shows the expected variation of density predicted by *Streltsov and Lotko* [2008]. Despite the overall low density values, the localized enhancement shown

around 09:54:04 UTC in Figure 2i amounts to an increase of about 50%, which does agree with the percent change predicted in the simulation results.

[17] The lack of electron flux seen in Figures 2c and 2d in the time range between 09:53:59 and 09:54:13 UTC may be attributed to the upwelling of a cold electron population. Figures 2g clearly shows that the drop in electron temperature corresponds well with the lack of electron flux in Figures 2c and 2d and the local density enhancement seen in Figure 2i. The strong Alfvénic precipitation, of largely downward-moving electrons, seen around 09:53:58 and 09:54:14 UTC appear to be intense enough to influence the net FAC. It is important to note that the stronger field perturbation, that seen around 09:54:14 UTC, actually occurs in a region of upward FAC (looking at Figure 2b). This is contrary to the model results of both *Streltsov and Lotko* [2008] and the new model presented here, which both predicted the small-scale waves inside the downward current region. However, this apparent offset between the FAC measurements and the fields may be attributable to a mix of temporal and/or spatial effects, either realistic or a result of the rocket's quick movement through the region.

[18] The presence of intense small-scale EM waves, observed in Figures 2e and 2f and in more detail in Figure 4, was stated previously as one of the observational characteristics of the IFI. These small-scale currents are generated in the ionosphere by the IFI, which is driven by the perpendicular electric field in the ionosphere. This field is produced by the closure of the larger-scale FAC through the ionosphere, and it maximizes on the boundaries of the magnetic FAC. This effect is described in detail by *Streltsov and Marklund* [2006] whose discussion of measurements performed by Cluster satellites did not focus on small-scale structures inside the IAR, and selected parameters of the magnetosphere-ionosphere system that do not include the presence of the IAR. However, their simulations explicitly show large-amplitude electric fields in the ionosphere on the boundaries of the downward current. In a later study, simulations by *Streltsov and Karlsson* [2008], which had a downward current region with upward currents on each side, yielded results that again showed small-scale structures existing throughout the downward current region, but with much greater intensity at the boundaries between the currents; the magnitude of the currents from *Streltsov and Karlsson* [2008] are similar to those seen by ACES-High. The model results from *Streltsov and Lotko* [2008] also predicted the small-scale structures to exist throughout most of the return current region, with greatest intensity at the equatorward edge of the downward current region. However, the data from ACES-High do not show the small-scale structures persisting throughout the downward FAC region, but only existing in localized regions near the boundaries of the return current region.

#### 5. Conclusion

[19] The ACES-High rocket obtained data as it passed through the upward and downward FAC regions associated with a discrete auroral arc in January 2009. Data from this rocket show evidence of small-scale electromagnetic waves in the downward FAC region, as predicted by the model of *Streltsov and Lotko* [2008] with some notable differences.

The ACES-High data found the small-scale electromagnetic waves existing in localized areas (roughly 10 km) near the equatorward and poleward boundaries of the downward current region, not existing throughout a majority of the return current region. The magnitude of the waves shown in the data is on the lower end of the range predicted by the model. The data from ACES-High show evidence of downward-moving Alfvénic precipitation associated with the small-scale structure. The region between the Alfvénic precipitation lacks significant electron flux.

[20] Analysis of the phase difference between the electric and magnetic fields of these small-scale waves and comparison with studies made by *Clemmons et al.* [2000] and *Knudsen et al.* [1992] have led to the conclusion that these oscillations are standing waves, either wholly or partially, created by reflection within the Alfvén resonator. The electron densities measured in the downward FAC region are up to an order of magnitude lower than would be expected compared to data from *Aikio et al.* [2004] and simulation results [*Streltsov and Lotko*, 2008; *Streltsov et al.*, 2011]. However, the enhancement does correlate to a roughly 50% increase in density, which agrees with the predictions made by *Streltsov and Lotko* [2008]. The measured increase in electron density inside the downward FAC region suggests that ACES-High flew through the area of enhanced density that *Streltsov and Lotko* [2008] predicted would be caused by the upward evacuation of plasma from the cavity created below.

[21] In response to these data from ACES-High, simulations were run using a model similar to that used by *Streltsov and Marklund* [2006], which decouples the FAC regions by launching only a single downward FAC region as opposed to an opposing pair (as done by *Streltsov and Lotko* [2008]). Results from this new simulation agree very well with the observations from ACES-High, showing small-scale electromagnetic waves with appropriate magnitudes appearing at the equatorward and poleward boundaries of the downward FAC region.

[22] In summary, this paper shows the following:

[23] 1. The ACES-High sounding rocket obtained the first in situ measurements of small-scale Alfvénic wave structures, evidence of the IFI, near the boundaries of the return current region associated with a discrete auroral arc.

[24] 2. These observations agree with the *Streltsov and Lotko* [2008] model that small-scale EM waves would be seen in the downward FAC region adjacent to a discrete auroral arc, and there would be an enhancement in plasma density at altitudes directly above the cavity as a result of plasma being evacuated upward. However, contrary to model predictions, the small-scale wave structures are only seen in localized areas of about 10 km near the boundaries of the return current region and not throughout it.

[25] 3. ACES-High observed increased density with a temperature characteristic of a cold ionosphere in the return current region; however, this density is still up to an order of magnitude lower than expected from simulations and other observations [*Streltsov and Lotko*, 2008; *Aikio et al.*, 2004]. This enhancement is consistent with the theory and results from *Streltsov and Lotko* [2008] that plasma is evacuated upward from lower altitudes to create a density cavity, another observational characteristic of the IFI, near a discrete auroral arc.

[26] 4. A new model, based on that by *Streltsov and Marklund* [2006], which decouples the FAC regions by launching only one downward current, has produced results very similar to the observations seen by ACES-High.

[27] **Acknowledgments.** The authors would also like to extend our gratefulness to the staff and engineers at NASA Wallops Flight Facility. The work in this paper was supported by several grants from the National Aeronautics and Space Administration: NNX07AK01G, NNX11AK71H, and NNX10AL17G to the University of New Hampshire; NNX12A144G and NNX10AL18G to Dartmouth College; and NNX07AJ97G to the University of Iowa.

[28] Robert Lysak thanks David Knudsen and another reviewer for their assistance in evaluating this paper.

## References

- Aikio, A., K. Mursula, S. Buchert, F. Forme, O. Amm, G. T. Marklund, M. Dunlop, D. Fontaine, A. Vaivads, and A. Fazakerley (2004), Temporal evolution of two auroral arcs as measured by the Cluster satellite and coordinated ground-based instruments, *Ann. Geophys.*, 22(1), 4089–4101, doi:10.5194/angeo-22-4089-2004.
- Atkinson, G. (1970), Auroral arcs: Result of the interaction of a dynamic magnetosphere with the ionosphere, *J. Geophys. Res.*, 75(2), 4746, doi:10.1029/JA075i025p04746.
- Clemmons, J. H., et al. (2000), Observations of traveling Pc5 waves and their relation to the magnetic cloud event of January 1997, *J. Geophys. Res.*, 105(A), 5441–5452, doi:10.1029/1999JA900418.
- Doe, R. A., M. Mendillo, J. F. Vickrey, L. J. Zanetti, and R. W. Eastes (1993), Observations of nightside auroral cavities, *J. Geophys. Res.*, 98(A1), 293–310.
- Kaeppler, S. R., et al. (2012), Current closure in the auroral ionosphere: Results from the auroral current and electrodynamic structure rocket mission, in *Auroral Phenomenology and Magnetospheric Processes: Earth and Other Planets, Geophysical Monograph Series*, vol. 197, edited by A. Keiling, E. Donovan, F. Bagenal, and T. Karlsson, pp. 183–192, American Geophysical Union, Washington, DC, doi:10.1029/2011GM001177.
- Kletzing, C. A., and S. Hu (2001), Alfvén wave generated electron time dispersion, *Geophys. Res. Lett.*, 28(4), 693–696, doi:10.1029/2000GL012179.
- Knudsen, D. J., M. C. Kelley, and J. F. Vickrey (1992), Alfvén waves in the auroral ionosphere: A numerical model compared with measurements, *J. Geophys. Res.*, 97(A1), 77–90.
- Lysak, R. L. (1991), Feedback instability of the ionospheric resonant cavity, *J. Geophys. Res.*, 96(A2), 1553–1568.
- Lysak, R. L., and Y. Song (2002), Energetics of the ionospheric feedback interaction, *J. Geophys. Res.*, 107(A8), 1160, doi:10.1029/2001JA000308.
- Mishin, E. V., W. J. Burke, C. Y. Huang, and F. J. Rich (2003), Electromagnetic wave structures within subauroral polarization streams, *J. Geophys. Res.*, 108, 1309, doi:10.1029/2002JA009793.
- Paschmann, G., S. Haaland, and R. Treumann (eds.) (2003), *Auroral Plasma Physics*, Kluwer Academic Publishers, Netherlands.
- Pokhotelov, O., V. Khrushev, M. Parrot, S. Senchenkov, and V. P. Pavlenko (2001), Ionospheric Alfvén resonator revisited: Feedback instability, *J. Geophys. Res.*, 106, 25813–25824.
- Shepherd, S. G., J. LaBelle, R. A. Doe, M. McCready, and A. T. Weatherwax (1998), Ionospheric structure and the generation of auroral roar, *J. Geophys. Res.*, 103, 29253–29266.
- Streltsov, A. V., and T. Karlsson (2008), Small-scale, localized electromagnetic waves observed by Cluster: Result of magnetosphere-ionosphere interactions, *Geophys. Res. Lett.*, 35, L22107, doi:10.1029/2008GL035956.
- Streltsov, A. V., and W. Lotko (2003a), Reflection and absorption of Alfvénic power in the low-altitude magnetosphere, *J. Geophys. Res.*, 108(A4), 8016, doi:10.1029/2002JA009425.
- Streltsov, A. V., and W. Lotko (2003b), Small-scale electric fields in downward auroral current channels, *J. Geophys. Res.*, 108(A7), 1289, doi:10.1029/2002JA009806.
- Streltsov, A. V., and W. Lotko (2004), Multiscale electrodynamic of the ionosphere-magnetosphere system, *J. Geophys. Res.*, 109, A09214, doi:10.1029/2004JA010457.
- Streltsov, A. V., and W. Lotko (2008), Coupling between density structures, electromagnetic waves and ionospheric feedback in the auroral zone, *J. Geophys. Res.*, 113, A05212, doi:10.1029/2007JA012594.

- Streltsov, A. V., and G. T. Marklund (2006), Divergent electric fields in downward current channels, *J. Geophys. Res.*, *111*, A07204, doi:10.1029/2005JA011196.
- Streltsov, A. V., T. R. Pedersen, E. V. Mishin, and A. L. Snyder (2010), Ionospheric feedback instability and substorm development, *J. Geophys. Res.*, *115*, A07205, doi:10.1029/2009JA014961.
- Streltsov, A. V., C.-L. Chang, J. Labenski, G. Milikh, A. Vartanyan, and A. L. Snyder (2011), Excitation of the ionospheric Alfvén resonator from the ground: Theory and experiments, *J. Geophys. Res.*, *116*, A10221, doi:10.1029/2011JA016680.
- Sydorenko, D., R. Rankin, and K. Kabin (2008), Nonlinear effects in the ionospheric Alfvén resonator, *J. Geophys. Res.*, *113*, A10206, doi:10.1029/2008JA013579.